MAX-PLANCK-INSTITUT FÜR PHYSIK UND ASTROPHYSIK
INSTITUT FÜR ASTROPHYSIK

THEORETICAL PROBLEMS IN HIGH RESOLUTION SOLAR PHYSICS

edited by

Hermann Ulrich Schmidt

Proceedings of the

MPA / LPARL*

Workshop

in München

16–18 September 1985

in preparation for the Solar Optical Telescope (SOT)

*MPA : Max-Planck-Institut für Astrophysik
LPARL: Lockheed Palo Alto Research Laboratories

Karl-Schwarzschild-Strasse 1 · 8046 Garching bei München

 POSITION PAPER:

Propagation of magneto-acoustic waves along solar flux tubes

P. Ulmschneider
Institut für theoretische Astrophysik
Im Neuenheimer Feld 561
6900 Heidelberg, Federal Republic of Germany

Abstract Time-dependent calculations of longitudinal waves in magnetic flux tubes are discussed. A comparison of adiabatic with non-adiabatic calculations demonstrates that radiation processes determine decisively the physical state in the tubes. Heating and mass motion produced by the waves depends strongly on the tube geometry. Fast spreading tubes are less heated. Long period waves show decreased heating and increased mass motion.

1. Introduction

In the last few years it has become clear that there is a strong observational correlation between the solar CaII K line brightness and the magnetic field strength. This ties in nicely with the stellar observations from IUE that rapidly rotating late-type stars which are presumably young and have greater magnetic field coverage show much greater MgII k line emission. Thus it appears well founded to assume that chromospheric heating is strongly tied to the magnetic field. High resolution observations indicate that the magnetic field on the solar surface is concentrated in very intense flux tubes outside which the atmosphere is virtually field free. This suggests that the chromospheric heating is done by magnetohydrodynamic waves propagating along flux tubes.

There are three principal mhd tube wave modes. The longitudinal or sausage mode is excited by compressing the tube. In this mode gas pressure is the main restoring force which makes the wave very similar to acoustic waves. The transverse or kink mode has as main restoring force magnetic tension produced by bending the magnetic field perpendicular to the tube axis. For the torsional waves the main restoring force is also magnetic tension which in this case is produced by azimuthal twist. It is very likely that all three wave modes are produced efficiently: for the case of longitudinal and transverse waves from buffeting of the flux tube by convection cells in the convection zone, see also Ulmschneider and Stein (1982); for torsional waves by a twisted shape of the magnetic field and by cyclonic downdrafts along the edges of the tube (Schüssler 1984). In any case it is very likely (see e.g. Hollweg et al. 1982) that strong nonlinear coupling lets modes go freely over into one another such that a single excited mode will produce the other modes as well.

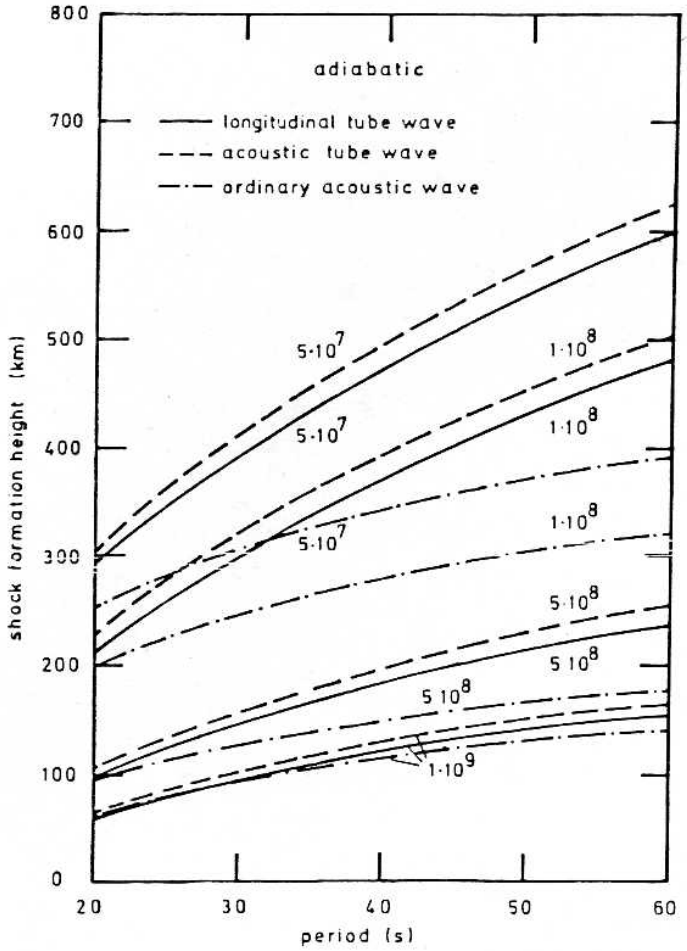

Fig.1 Shock formation heights for various wave types

2. Adiabatic calculations.

For longitudinal waves Herbold et al. (1985) have made a detailed comparison with acoustic tube waves and ordinary acoustic waves. These three waves are described by the same set of hydrodynamic equations. The only difference is in the way the tube cross section A varies. For longitudinal waves in the thin tube approximation the cross section is given by

$$A(x,t) = \phi_M/(8\pi(p_E(x)-p(x,t))^{1/2} \qquad (1)$$

where ϕ_M is the constant magnetic flux, p the gas pressure and $p_E(x)$ the gas pressure of the external medium as function of height. Acoustic tube waves have a cross section A(x) independent of time, while ordinary acoustic waves can be thought of as tube waves of constant cross section.

The differences between these waves become especially apparent when the nonlinear behaviour is compared for large amplitudes. For adiabatic calculations Fig.1 shows the height of shock formation for waves of various period (s) and energy flux (erg cm^{-2} s^{-1}). A tube of diameter 114 km

with field strength 1560 G at height zero was taken. It is seen that acoustic tube waves and longitudinal waves are very similar. The differences are mainly due to the different initial velocity amplitude of the two waves when the same initial flux

$$F_M = 1/2\ \varrho_0 c_0 u_0^2 \qquad (2)$$

is taken. Here ϱ_0 is the density, u_0 the velocity amplitude and c_0 the propagation speed at zero height. Since the propagation speed c_T for longitudinal waves is much smaller than the sound speed these waves have greater initial amplitude u_0, which generates shocks at somewhat lower height. Constant tube cross section leads to the very different behaviour of ordinary acoustic waves where shocks form much more rapidly at low height.

3. Radiatively damped waves, methods

Small amplitude transverse or torsional waves do not have gas pressure and temperature fluctuations. Thus radiation is not important for these waves. For all other cases, e.g. large amplitude transverse and torsional waves and especially longitudinal waves, radiation is a decisive property in the wave propagation. Vernazza et al. (1981) have shown that the main chromospheric emitters are the H^- continuum, the principal lines of CaII and MgII, the Lyman continuum and the Lyman α line. H^- contributes mainly in the photosphere and temperature minimum area while Lyman emission occurs only in the high chromosphere. Deeper in the photosphere a multitude of metal line and continuum emitters provide contributions which can be computed using Kurucz's (1979) opacity tables.

As the gas pressure in the flux tube is considerably smaller than the external pressure the optical depth in the tube is much smaller. In the photosphere above about 100 km height the typical flux tube is optically thin for the emitters collected in the Kurucz table. Here a gas element of a thin tube is bathed in a radiation field of mean intensity $J_\nu(x)$ produced outside the tube. Herbold et al. (1985) have used a grey $J(x)=\sigma T_E^4/\pi$ where $T_E(x)$ is the external temperature, while Schmitz et al. (1985) have used a specified non-grey (19 frequency points) surface intensity J_ν independent of height which is valid for heights greater than 300 km. In these cases radiation becomes a local function of temperature and pressure.

The situation is more complicated when CaII and MgII lines are considered (Ulmschneider and Muchmore 1986). Here optical depths can be large. In typical flux tubes one finds

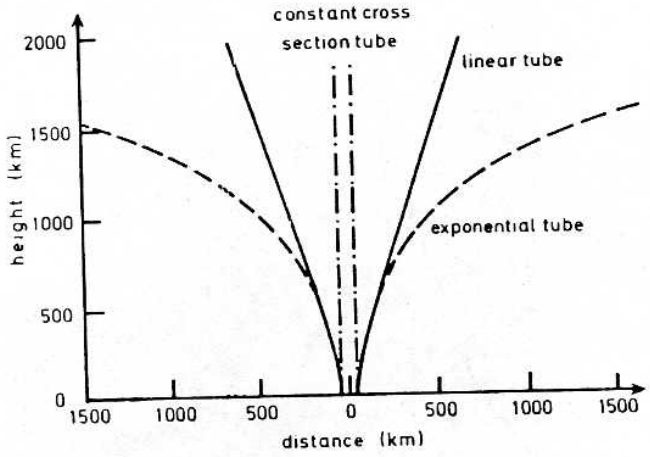

Fig.2 Types of flux tube geometry considered

that the optical depth across the tube is much larger than along the tube. Thus a plane parallel transfer calculation should be a good approximation. To make the method tractable for time-dependent calculations numerous assumptions had to be made. The atomic model e.g. for MgII k has been simplified to two bound levels. The net radiative cooling rate (erg $cm^{-3}s^{-1}$) neglecting stimulated emission is then given by

$$\phi_R = h\nu_{12} n_1 B_{12} \varepsilon (B_{\nu 12} - S_{12}) \qquad (3)$$

where $h\nu_{12}$ is the photon energy, $n_1 B_{12}$ the absorption rate.

$$\varepsilon = n_E \Omega_{21} / A_{21} \qquad (4)$$

is the photon destruction probability which is a function of the electron density only (Ω_{21} and A_{21} being constants). $B_{\nu 12}$ is the Planck function and S_{12} the source function. To account for the neglected emitters (MgIIh and CaIIH+K+IRT lines) the MgII results were subsequently scaled by a factor 7. Complete redistribution was assumed which considerably overestimates the emission. The statistical rate equations were solved under the assumption that populations attain their values instantaneously. Hydrogen ionization was not considered in the hydrodynamics but included in LTE in the computation of the electron density for the radiation treatment. The ionization of e.g. MgI to MgII and of MgII to MgIII was computed in LTE. The coupled set of line radiative transfer equations (with 29 frequency points) and the statistical rate equation was solved using the core-saturation method of Kalkofen and Ulmschneider (1984). To compare our method with the more elaborate static calculations we have recomputed the chromospheric emission rates of model C of Vernazza et al. (1981). As expected our method gave more emission by about a factor of ten.

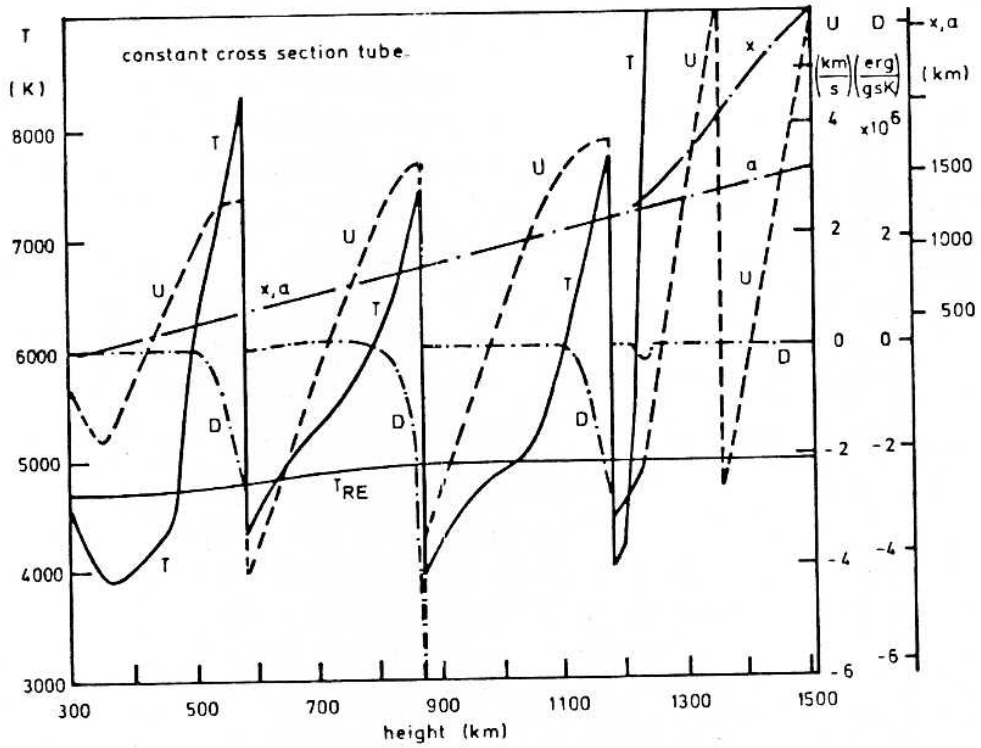

Fig.3 Temperature T, velocity u, damping function D, Euler x and Lagrange a heights for an acoustic wave in a tube of constant cross section. T_{RE} indicates initial radiative equilibrium temperature. The wave has a period of 45 s and flux 2.5E7 erg $cm^{-2}s^{-1}$ and is shown at time 1772 s

Subsequent scaling was applied such that our method now reproduces Vernazza et al.'s total chromospheric emission.

5. Radiatively damped waves, results

Fig. 2 shows the different types of flux tubes taken in the wave calculations by Ulmschneider and Muchmore (1986). We took a tube of constant cross section with magnetic field strength 1500 G and diameter 100 km. The linear tube spreads first exponentially up to 500 km and thereafter linearly. The exponential tube spreads exponentially throughout the atmosphere. Fig.'s 3,4,5 respectively show a calculation along the tube of constant cross section representing an ordinary acoustic wave calculation, an acoustic wave calculation along a linear tube, and along an exponential tube. These computations were made with the same wave period 45 s and the same energy flux F_M = 2.5E7 erg $cm^{-2}s^{-1}$.

It is seen that due to energy conservation the wave amplitudes depend strongly on the geometry. At about 570 km the constant case has a temperature T=8300 K and a velocity u=3.0 km/s. Both the linear and exponential case have T=5800 K and u=1.7 km/s because these waves up to this height propagate in the same tube. At 1300km the linear case has T=7100 K and

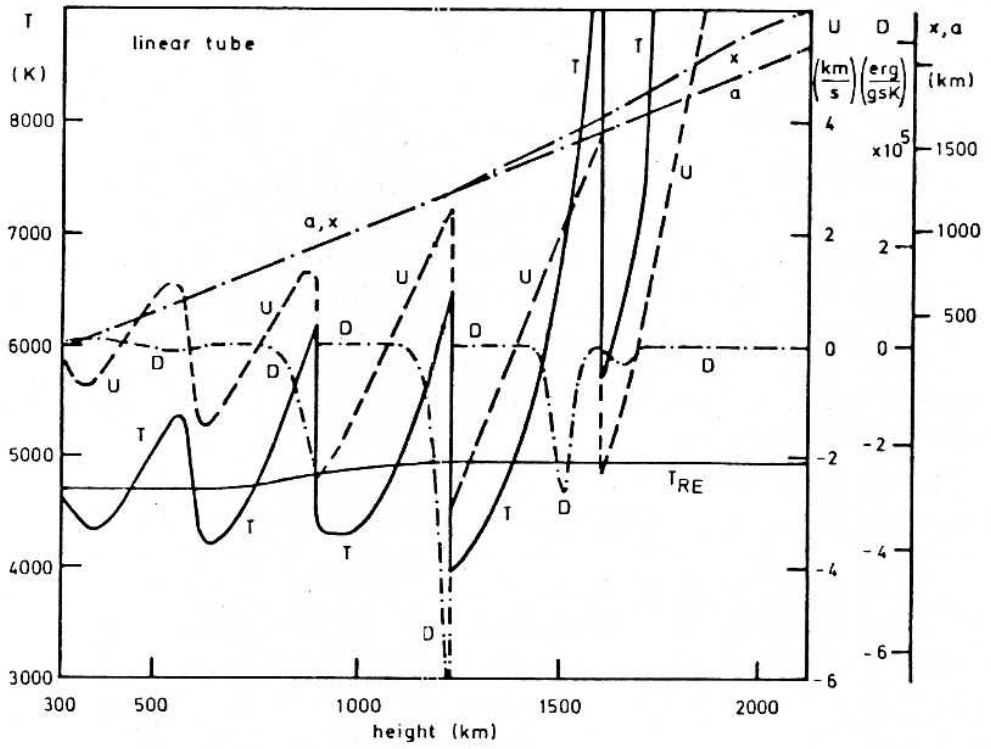

Fig.4 Same as Fig.3 but for a linear tube at time 332 s

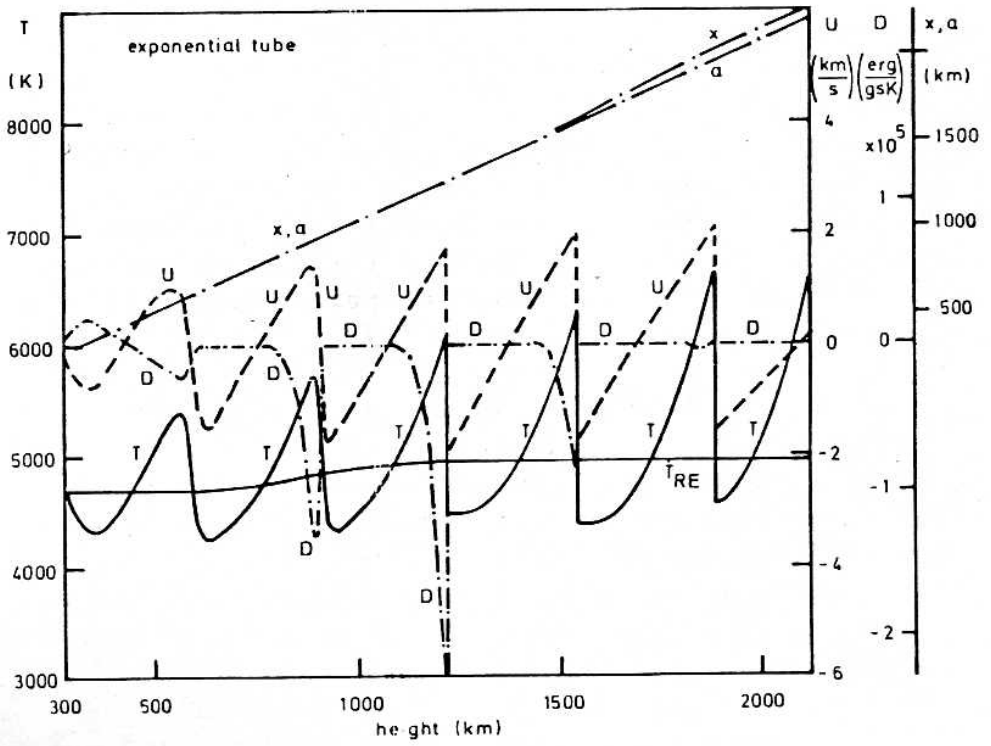

Fig.5 Same as Fig.3 but for an exponential tube at time 693 s

u=2.8 km/s and the exponential T=6500 K and u=1.9 km/s. The larger the tube spreading the smaller the amplitudes.

Fig.'s 3 to 5 also show the radiative damping function D which is related to the net radiative cooling rate by $D=-\phi_R/\vartheta T$. The different wave amplitudes produce large differences in emission. This is due to the fact that according to equ. (4) both ϵ (as function of n_E) and $B_{\nu 12}$ depend strongly on temperature. The source function is small and a slowly varying function of height. The emission is concentrated in intense radiation layers behind the shock. In front of the shock ϵ is many orders of magnitude smaller resulting in negligible absorption.

At greater height depending on pressure and temperature MgII gets ionized to MgIII. This destruction of the only remaining emitter leads to the fact that the shock dissipation becomes unbalanced. This leads to a rapid rise of the mean temperature eventually resulting in a transition-layer. The position of the transition layer depends strongly on the tube geometry. In the constant tube case the transition layer height is x_{TR}=1300 km, in the linear case x_{TR}=1800 km, in the exponential case x_{TR}=2500 km. In all calculations, even those with MgII emission neglected (c.f. Herbold et al. 1985), we found transition layers. Note that our usage of the term transition layer applies to a rapid temperature rise. The observed transition layer is probably produced similarly by the ionization of hydrogen.

As the dissipated energy can not be radiated away it is put into mass motion. Thus mass motion depends strongly on the tube geometry. This can be seen in the Figures e.g. as displacement of the Eulerian height from the Lagrangian height of the topmost mass point. Large mass motion is produced in the constant tube; comparatively little in the exponential tube.

For the linear tube Fig. 6 shows an acoustic wave of period 90 s and the same wave energy. It is seen that mass motions are greatly increased. This is due to the fact that longer period waves produce stronger shocks and generate transition layers at lower heights. Long period waves put more energy into mass motion and less into chromospheric heating.

6. Conclusions

Radiation processes occuring in longitudinal and large amplitude transverse and torsional waves determine decisively the physical state in the flux tube. These processes depend strongly on the geometry of the flux tube. Exponentially spreading tubes have small chromospheric

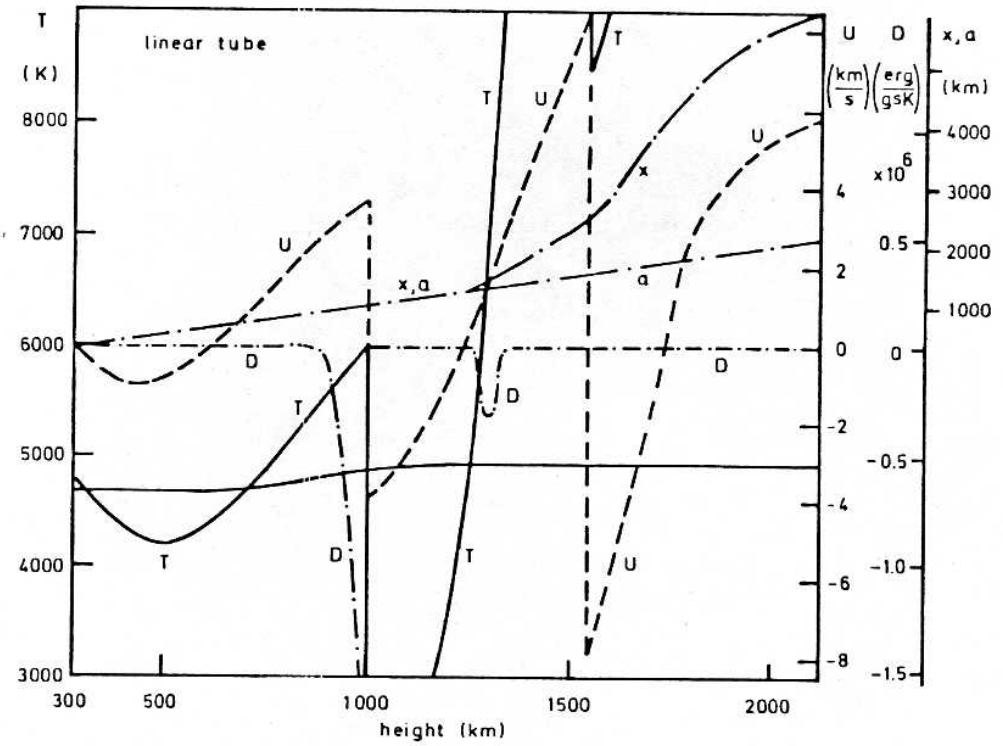

Fig.6 Same as Fig.3 but for a linear tube and a wave period 90s at time 490 s

temperature rises, low radiative emission, transition layers at great height and small mass motion. For linearly spreading tubes and even more so for constant cross section tubes the opposite is true. Larger wave period increases mass motion and decreases heating.

References

Herbold, G., Ulmschneider, P., Spruit, H.C., Rosner, R.: 1985, Astron. Astrophys. 145, 157.

Hollweg, J.V., Jackson, J., Galloway, D.: 1982, Solar Physics 75, 35.

Kalkofen, W., Ulmschneider, P.: 1984, Methods in radiative transfer, W. Kalkofen ed., Cambridge, p.131.

Kurucz, R.: 1979, Astrophys. J. Suppl. 40, 1.

Schmitz, F., Ulmschneider, P., Kalkofen, W.: 1985, Astron. Astrophys. 148, 217.

Schüssler, M.: 1984, Astron. Astrophys. 140, 453.

Ulmschneider, P., Muchmore, D.: 1986, Astron. Astrophys., to be published.

Ulmschneider, P., Stein, R.F.: 1982, Astron. Astrophys. 106 9.

Vernazza, J.E., Avrett, E.H., Loeser,R.: 1981, Astrophys. J. Suppl. 30, 1.